Record-dynamics description of spin-glass thermoremanent magnetization: A numerical and analytical study

Paolo Sibani and Jacob Møller Kirketerp
FKF, University of Southern Denmark, Campusvej 55, DK5230, Odense M, Denmark

(Received 23 June 2020; accepted 9 October 2020; published 26 October 2020)

Thermoremanent magnetization data for the three-dimensional Edwards-Anderson (EA) spin glass are generated using the waiting time method as a simulational tool and interpreted using record dynamics. We verify that clusters of contiguous spins are overturned by quakes, nonequilibrium events linked to record-sized energy fluctuations, and we show that quaking is a log-Poisson process, i.e., a Poisson process whose average depends on the logarithm of the system age, counted from the initial quench. Our findings compare favorably with experimental thermoremanent magnetization findings and with the spontaneous fluctuation dynamics of the EA model. The logarithmic growth of the size of overturned clusters is related to similar experimental results and to the growing length scale of the spin-spin spatial correlation function. The analysis buttresses the applicability of the waiting time method as a simulational tool, and of record dynamics as a coarse-graining method for aging dynamics.

DOI: 10.1103/PhysRevE.102.042131

I. INTRODUCTION

The multiscale relaxation process called *aging* is observed in, e.g., spin-glasses [1–3], colloidal suspensions [4,5], vortices in superconductors [6], and evolving biological and cultural ecologies [7–9]. Important aspects of aging phenomenology have been elucidated by spin-glass linear response experiments [1–3], including thermoremanent magnetization (TRM) studies of memory and rejuvenation effects [1,10–12], subaging, and end of aging behavior [13,14]. Numerical simulations [15–20] of the Edwards-Anderson (EA) model [21] provide additional insight and a test of theoretical assumptions.

In TRM experiments, the system is thermalized in a magnetic field H and then thermally quenched at time $t = 0$ (here we gloss over the fact that an instantaneous quench is not experimentally achievable) below T_c, the spin-glass critical temperature. At $t = t_w$ the field is cut and the magnetization decay is measured for $t > t_w$. Note that field removal and time origin are usually taken to coincide, in which case t notationwise corresponds to our $t - t_w$.

Record dynamics [22,23] (RD) deals with complex systems [24] lacking time translational invariance and evolving through a series of equilibrium-like configurations of increasing duration. This experimental and/or observational background can be theoretically associated with a hierarchy of dynamical barriers and, in a second step, with a hierarchy of nested ergodic components [25], each predominantly found in a stationary, or pseudoequilibrium, state.

RD highlights the irreversible events, called *quakes*, bringing the system from one pseudoequilibrium state to the next. It posits that quakes constitute a Poisson process whose average depends on the logarithm of time, for short a log-Poisson process. The transformation $t \to \ln t$ then produces a log-time homogeneous coarse-grained description of aging, yielding specific predictions for experimental and numerical observations.

An analysis of experimental TRM data [26] and simulations of the zero-field-cooled magnetic linear response of the three-dimensional (3D) EA model with Gaussian couplings [17] make use of RD, and they identify quakes as anomalously large magnetic fluctuations. More recently [20], the same model was simulated for a range of low temperatures in zero field, with the waiting time method (WTM) [27] as a simulational tool. Quakes are associated with records in the time series of energy values produced by the simulation, and real-valued event times are assigned to them, providing the statistics needed to ascertain the log-Poissonian nature of the quaking process.

Following the same methodology, the present study aims to show the agreement between WTM simulations and experimental descriptions, and the ability of RD to predict the key features of spin-glass dynamics. To this end, we first demonstrate the log-Poisson nature of the quaking process, and then we check RD predictions on the time dependence of the TRM and the system excess energy [17,26], Finally, the real-space effect of quakes is described in terms of the near simultaneous overturning of a cluster of adjacent spins, i.e., a spin-flip cascade over a barrier. This is compared with experimental results, where clusters of a similar nature are extracted from TRM traces [28].

The rest of the paper is organized as follows: In Sec. II the model and the simulation method are briefly described. Section III is devoted to the simulation results, and Sec. IV to a summary and a conclusion.

II. MODEL AND SIMULATION PROTOCOL

This section closely follows Ref. [20], to which we refer for additional details. Essential information, including

differences from the above reference, are given here for the reader's convenience.

We consider an Ising EA spin glass [21] placed on a cubic grid with linear size $L = 20$ and periodic boundary conditions. Each of the 2^N configurations is specified by the value of $N = L^3$ dichotomic spins, and has, in a magnetic field H, an energy given by

$$\mathcal{H}(\sigma_1, \sigma_2, \ldots, \sigma_N) = -\frac{1}{2}\sum_{i=1}^{N}\sum_{j\in\mathcal{N}(i)} J_{ij}\sigma_i\sigma_j - H\sum_{i=1}^{N}\sigma_i, \quad (1)$$

where $\sigma_i = \pm 1$ and where $\mathcal{N}(i)$ denotes the six nearest neighbors of spin i. For $j < i$, the J_{ij}'s are drawn independently from a Gaussian distribution with zero average and unit variance. Finally, $J_{ij} = J_{ji}$ and $J_{ii} = 0$. All parameters are treated as dimensionless. For $H = 0$, the model has a phase transition from a paramagnetic to a spin-glass phase at a critical temperature, which in Ref. [29] is estimated to be $T_c = 0.9508$.

Our system is thermalized at temperature $T_0 = 3$ in a magnetic field $H = 0.1$, instantaneously quenched at time $t = 0$ to temperatures $T = 0.5, 0.6, \ldots, 1$, and then left to age isothermally. At time t_w, the magnetic field is removed and the magnetization decay is observed as a function of time. We consider three values of t_w: 10, 100, and 200.

The real-space manifestation of the quakes in the EA model are cascade events, where clusters of adjacent spins flip coherently. The distinction between cascade events and scattered flips is moot in standard MC algorithms, e.g., parallel tempering [30], since consecutive queries are always spatially uncorrelated, and the shortest available "time" scale is a MC sweep. The rejectionless waiting time method (WTM) [27], where "waiting time" refers to the time between two successive moves, generates a Markov chain closer to a physical relaxation process than is the case for standard MC algorithms.

Each basic degree of freedom, e.g., a spin i, performs a Poisson process whose characteristic timescale τ_i depends on the interactions with its neighbors. Any state change of the neighbors resets the process and requires the recalculation of τ_i. Every spin has a flip time at which it would flip if nothing else happened, and the spin that actually flipped is the one with the earliest flip time. Each spin flip in a simulation is thus associated with an intrinsic real-valued time variable t, and spatially and temporally localized dynamical events are possible and can be precisely identified.

When the WTM is applied to the EA model, spin i stays put for an exponentially distributed time interval τ_i, unless one of its neighbors flips. The mean waiting time τ_i to its next possible move hinges on the energy change ΔE_i such a move would entail. Assuming $\Delta E_i > 0$, the situation is locally metastable, but an updated value of ΔE_i due to activity in the neighborhood requires a recalculation of the waiting time. In the unstable situation in which $\Delta E_i < 0$, the waiting time is with high probability very short and the spin quickly flips. A flip can in turn create a new unstable situation in the neighborhood, and iterating this process generates a sequence of neighboring spins quickly flipping one after the other. When no further energy loss is possible, the process stops and a new metastable configuration is created differing from its predecessor in the orientation of a spatially connected cluster of spins.

To detect a quake, we follow Ref. [20] and use two "record" energy values in combination with a subdivision of the time axis in short intervals of equal duration δt. The quantity $E(t)$ is the energy as a function of time. The two record values used are the "best so far" energy $E_{\rm bsf}(t)$ and the "highest so far" energy $E_{\rm h}(t)$. The former is the least energy seen during the simulation up to the "current" time t,

$$E_{\rm bsf}(t) = \min_{0<t'<t}(E(t')), \quad (2)$$

and the latter is the largest energy value seen, relative to the best so far energy,

$$E_{\rm h}(t) = \max_{0<t'<t}(E(t') - E_{\rm bsf}(t')). \quad (3)$$

For simplicity, the system energy E is measured relative to $E_{\rm bsf}$ and its current position on the time axis is continuously tracked. A quake alert device with three states 0, 1, and 2 is utilized for quake identification. State 0 covers standard fluctuation dynamics, state 1 is reached when $E_{\rm h}$ is updated, i.e., increased, and state 2 is reached when $E_{\rm bsf}$ is subsequently updated, i.e., decreased. At this point, an unfolding quake is detected and the alert level is reset to 0. The quake event is deemed to have terminated once time exceeds the boundary of the current δt subinterval of the time axis. The spin cluster that changed orientation during the quake is identified, and the time at which the quake occurred is registered. In [20], the same procedure is followed except that the detection device there has two states rather than three. State 1, which triggers quake detection, is reached if either $E_{\rm h}$ or $E_{\rm bsf}$ is updated. We modified the algorithm to avoid an excessive number of events being registered right after magnetic field removal.

III. RESULTS

A. Log-Poisson statistics

In this section, we show that the quakes extracted from our TRM data, i.e., after field removal at times $t_1 < t_2 \cdots < t_k \cdots$, with $t_1 > t_w$, are a Poisson process whose average depends on the logarithm of t_k/t_{k-1}. Since the analysis deals with the distribution of inter-quake times, the waiting time t_w does not explicitly enter the discussion.

A quake that flips a cluster can facilitate the overturning of a partly overlapping or neighboring cluster. Quakes can therefore be interdependent in regions of configuration space extending well beyond the correlation length associated with thermal equilibrium fluctuations.

In a large system, quake to quake correlations, not to be confused with thermal correlations, will eventually die out and temporally close, but spatially distant successive quakes will then be uncorrelated. We focus on a spatial domain where quakes are all interdependent, and where the transformation $t \to \ln t$ captures all temporal correlations. Quaking is then described by a memoryless Poisson process whose average is proportional to the logarithm of time, i.e., a log-Poisson process.

To ascertain if this is actually the case, it suffices to check whether the log-waiting times between successive events have an exponential PDF with unit average. Log-waiting times are

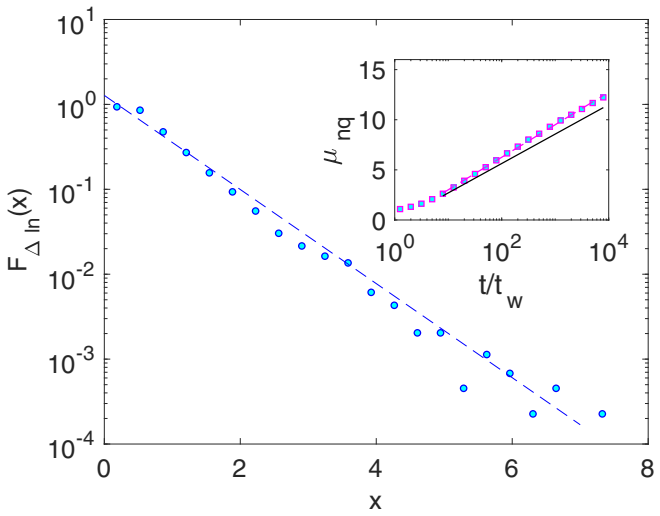

FIG. 1. Symbols: PDF of "logarithmic waiting times" $\Delta\ln$, for the aging temperatures $T = 0.5$. Dotted line: fit to the exponential form $y(x) = r_q e^{-r_q x}$ with $r_q = 1.275$. Inset: the squares show the average number of quakes vs the logarithm of t/t_w for $t_w = 10$. The hatched line depicts the fitted function $y = r'_q \ln t - 0.2388$ with $r'_q = 1.410$ while the full line makes use of the logarithmic rate r_q. The fact that $r'_q \neq r_q$ shows a discrepancy between the two estimates of the logarithmic rate of events.

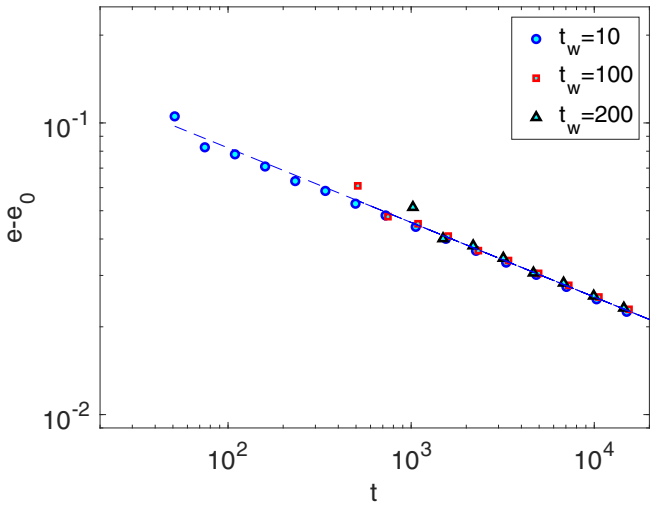

FIG. 2. Symbols: the energy per spin, with a fitted ground-state energy value subtracted, is plotted vs time for three systems with different field removal times. The dotted line is a fit to the power law $y(t) = at^{-\alpha}$, where a and α are free parameters.

simply defined in terms of the occurrence time t_k of the kth quake as $\tau_k = \ln(t_k/t_{k-1})$. Their empirical PDF is predicted to have the form

$$F_{\Delta\ln}(x) = r_q e^{-r_q x}, \tag{4}$$

where the constant r_q, the logarithmic quaking rate, is unity. As shown in the main panel of Fig. 1, the exponential PDF fits our data, though with a value of r_q somewhat higher than predicted. The inset of the same figure shows that the number of quakes that fall in the interval $(0, t]$, averaged over all trajectories, grows as $\mu_{nq}(t) = r'_q \ln(t)$. The logarithmic growth is as predicted by RD, but $r'_q > r_q$ while $r_q = r'_q$ according to theory. The two lines in the inset of Fig. 1 highlight the difference.

To conclude this section, briefly consider the situation in which (4) does not fit the empirical distribution of log-waiting times. Plainly, the discrepancy can arise if RD does not apply to the problem at hand. The other possibility is that data are collected over a spatial domain large enough to accommodate uncorrelated quakes. In this case, the average number of quakes will still grow logarithmically, with a prefactor reflecting the number of uncorrelated domains contained in the system. Since the waiting time between uncorrelated events is exponentially distributed, once uncorrelated quakes dominate, the PDF of waiting times—rather than log-waiting times—between successive quakes will be exponential. To recover Fig. 1, one needs to consider domains of reduced size. Reference [5] gives an example in which this situation arises. Alternatively, one can follow Ref. [31] and note that uncorrelated quakes produce a peak in $F_{\Delta\ln}(x)$ for small waiting times near $x = 0$. For sufficiently large x, the decay remains unchanged, i.e., exponential.

B. Macroscopic data

Unlike experiments, numerical simulations provide easy access to the system energy. Figure 2 shows the difference $e(t) - e_0$ between the energy per spin and its ground-state value plotted versus time t. Three data sets are included, corresponding to different values of t_w, all three fitted to the same power law,

$$e(t) - e_0 = at^{\lambda_e}, \tag{5}$$

where $e_0 = -1.6813$, $a = 0.2664$, and $\lambda_e = -0.2557$ are fitting parameters. As expected, in a linear response experiment no significant energy dependence appears on the field removal time t_w.

Equation (5) was proposed in [32] to estimate the ground-state energy e_0 as the value producing the power-law decay. The decay was observed in isothermal simulations of the EA model, using the WTM [17] and parallel tempering [18]. See Eq. (31) and Table 5 of the latter reference for the correspondence to the present notation. These authors tentatively attribute the power-law decay to the system being critical for a range of temperatures. Our estimate $e_0 \approx -1.68$ is nearly identical to that of [17], while Ref. [18], where much larger systems are considered with two-valued couplings $J_{i,j} = \pm 1$, finds values close to -1.77. The exponent λ_e is a negative and linearly decreasing function of temperature, with the value $\lambda_e(T = 0.5) \approx -0.25$ from [17] close to our current estimate. Reference [18] finds $\lambda_e(T = 0.6) = -0.193$ somewhat higher than our $T = 0.5$ value. The mismatch is related to algorithmic details. Note, however, that [17] and [18] agree on λ_e being a decreasing function of T.

Our main interest lies not in how to best estimate the ground-state energy, but in the fact that RD predicts the power-law decay, in a way unrelated to critical behavior. Assuming that only quakes can lower the energy, $e(n)$ is a function of the number n of quakes occurring in the interval (t_w, t). Furthermore, each quake can be expected to decrease the energy difference $\Delta_e(n) = e(n) - e_0$ by a constant fraction.

Our assumption entails

$$\Delta_e(n) = \Delta_e(0)x^n, \tag{6}$$

with $0 < x < 1$. To extract a time dependence, the expression must be averaged over the Poisson distribution of the number of quakes falling in the observation interval (t_w, t).

Taking $\Delta_e(t) = e(t) - e_0$, this yields

$$\Delta_e(t) = \Delta_e(t_w)\left(\frac{t}{t_w}\right)^{-r_q} \sum_{n=0}^{\infty} \frac{[x r_q \ln(t/t_w)]^n}{n!}$$

$$= \Delta_e(t_w)\left(\frac{t}{t_w}\right)^{-r_q(1-x)}. \tag{7}$$

In an RD description, the exponent λ_e characterizing the energy decay is given by $\lambda_e = -r_q(1-x)$, which is unrelated to any critical exponent. Power-law behavior comes indeed naturally in processes involving activation over a *hierarchy* of barriers; see [33] and references therein.

Turning now to the thermoremanent magnetization (TRM), we use the gauge transformation $\sigma_i \to \sigma_i(t_w)\sigma_i$, $J_{ij} \to \sigma_i(t_w)\sigma_j(t_w)J_{ij}$ to map it into the correlation function

$$C(t_w, t) = \sum_i \langle \sigma_i(t_w)\sigma_i(t)\rangle. \tag{8}$$

Modulo multiplicative constants, the two functions hold equivalent information, and since the general form of the autocorrelation function is theoretically available, we can use it to fit the TRM.

We consider the decorrelation induced by the quakes, which allow the system to equilibrate in increasingly large ergodic components. Quaking is a log-time homogeneous stochastic process, involving a set of interacting mesoscopic dichotomic variables, i.e., our clusters. Even though a formal description of how clusters interact is lacking, general arguments [24] lead to

$$C(t_w, t) = \sum_i w_i \exp\left(\lambda_i \ln(t/t_w)\right), \tag{9}$$

where the λ_i's are negative eigenvalues associated with the normal modes of the relaxation process, and all w_i are positive real numbers.

TRM time series are plotted in Fig. 3 as symbols versus the scaled time t/t_w. Neglecting small deviations from pure aging [10], all data are fitted by the same function, represented by a staggered line and obtained by truncating Eq. (9) to two terms, each having the form $w_i t^{\lambda_i \frac{t}{t_w}}$. The fitted exponents are $\lambda_1 = -0.167$ and $\lambda_2 = -5.418$ with prefactors $w_1 = 0.022$ and $w_2 = 30.83$. The first term is well approximated by a logarithm for the range of the abscissa, while the second only matters for values of the latter close to 1. Note that power laws eventually vanish. This ensures that TRM traces with different t_w values approach both zero and each other when plotted as a function of the observation time $t_{obs} = t - t_w$. This feature has been measured experimentally in [14], where it was termed "end of aging." Figure 4 shows six TRM traces, taken for $t_w = 10$ at temperatures $T = 0.5, 0.6, \ldots, 1$, with the staggered line depicting fits based, as before, on Eq. (9). The exponent closest to zero is plotted in the inset versus the temperature T, on which it has the linear dependence shown by the line

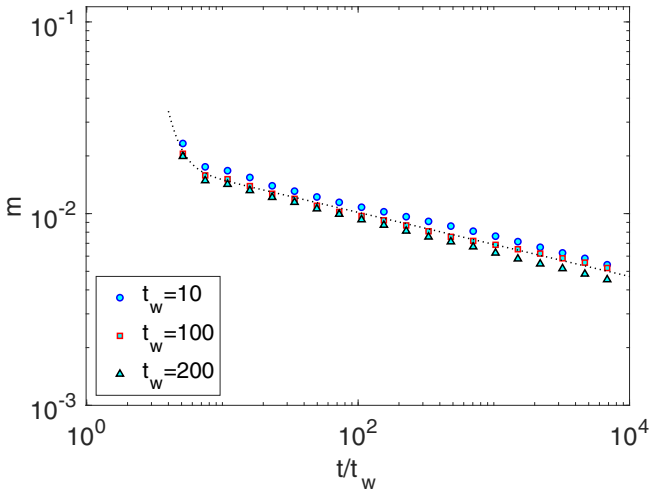

FIG. 3. Symbols: Thermoremanent magnetization data for $T = 0.5$ plotted vs scaled time t/t_w. Three data sets are shown corresponding to the t_w values given in the legend. Dotted line: fit using two terms of the expansion (9).

$-\lambda_1 = 0.33T$. Finally, note that our earlier RD analysis of TRM experiments [23] is also based on Eq. (9), but it utilizes three rather than two of its terms. The dominant exponent there is closer to zero and almost temperature-independent, which produces a near logarithmic TRM decay.

C. Mesoscopic real-space properties

The size of thermally correlated domains has attracted both numerical [15,16,18,19,34,35] and experimental [28,36] attention. As the aging process surmounts increasingly high free-energy barriers, and thermal equilibrium is reached in

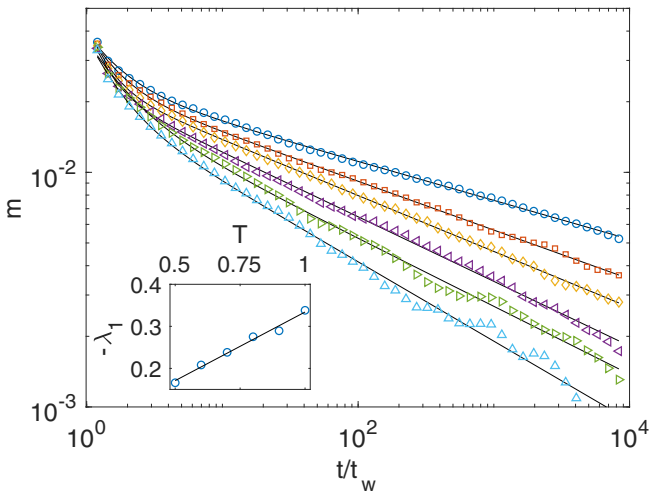

FIG. 4. Symbols: Thermoremanent magnetization data for isothermal aging at temperature T. From top to bottom, data sets collected at $T = 0.5$, 0.6, 0.7, 0.8, 0.9, and 1 are plotted vs the scaled time t/t_w, where $t_w = 10$. Dotted lines: fits using two terms of the expansion (9). Inset: the exponent of the dominant term in the expansion is plotted vs the temperature T. The line is the linear fit $-\lambda_1 = 0.33T$.

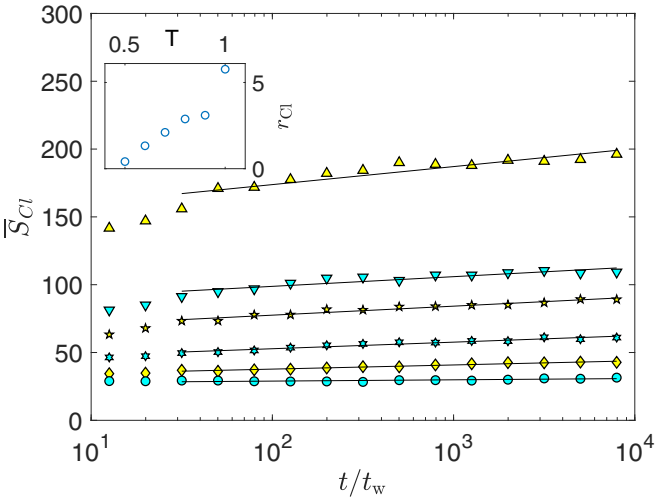

FIG. 5. Symbols: the average cluster size $\overline{S}_{\rm cl}$ is plotted vs the scaled time $t/t_{\rm w}$ for different temperatures T and $t_{\rm w} = 10$. From top to bottom, the data sets are collected at $T = 1$, 0.9, 0.8, 0.7, 0.6, and 0.5. The lines are linear fits of $\overline{S}_{\rm cl}$ to $\log t/t_{\rm w}$. The inset depicts the corresponding logarithmic rates vs the temperature T.

increasingly larger ergodic components, the domain size is expected to grow. The process has been followed by measuring the correlation length $\xi(t, T)$ associated with the spin-spin correlation function [15,16], by identifying spatial domains using projections on an alleged ground state obtained by annealing [34,35], or, experimentally, by an analysis of TRM data introduced by Joh *et al.* [28]. The method follows $S(t_{\rm obs})$, the derivative of the TRM with respect to the logarithm of the observation time, in our notation $t_{\rm obs} = t - t_{\rm w}$, and in particular the position of its maximum, which demarcates the crossover at $t_{\rm obs} = t_{\rm w}$ from pseudoequilibrium to nonequilibrium dynamics. Increasing the applied field reduces the corresponding free-energy barriers, and thereby shifts the maximum of $S(t_{\rm obs})$ to the left by an amount proportional to the size of the spin clusters participating in the barrier-crossing process.

These clusters are observed directly in numerical simulations, here and in [20], as the coherent movement of adjacent spins triggered by a quake. To obtain the size of clusters flipped "near" a certain time t, the simulation time is subdivided into 41 bins of equal logarithmic duration. Choosing t at the boundary between two bins, all clusters overturned at times within these bins are assigned to t.

Figure 5 depicts the average size $\overline{S}_{\rm cl}$ of clusters flipped near time t versus the scaled time variable $t/t_{\rm w}$ for $t_{\rm w} = 10$ and temperatures, from top to bottom, $T = 1$, 0.9, 0.8, 0.7, 0.6, and 0.5. The lines are fits showing the logarithmic growth of the cluster size, and the corresponding rates are plotted in the inset versus the temperature T. The statistics is obtained using 1000 independent simulations for each parameter value. The data can be fitted by the expression

$$S_{\rm Cl}(t, T) = (aT + b)\ln(t/t_{\rm w}) + C, \tag{10}$$

where $a = 9.3937$, $b = -4.445\,69$, and C is a constant. Clearly, the logarithmic growth rate should never be negative, and our linear fit is inadequate for temperatures below $T = 0.5$.

To connect the cluster size to the correlation length $\xi(t, T)$ requires theoretical assumptions [19,28], which, however, seem hard to verify unequivocally. The difficulty arises because correlation lengths of all origins, even when observed for long time intervals, only have a modest variation, typically spanning less than a decade. Furthermore, a simple dimensional connection between correlation length and the average size of flipped clusters could be strongly affected by the spatial heterogeneity, since all spins participate in reversible thermal fluctuations, but many are not involved in quakes at all.

Reference [16] shows that both a power law and a logarithm can fit the time dependence of the correlation length $\xi(t, T)$ for the EA model with Gaussian bonds, and [36] collects and discusses results from many different sources, all fitted using two power laws, with small exponents linearly dependent on the ratio of the temperature to its critical value.

The time dependence of the cluster sizes extracted from experimental data is shown in [28], on a linear scale versus a logarithmic timescale in their Fig. 4 and on a log-log scale in their Fig. 5. Assuming that the characteristic cluster size is the third power of the correlation length, $S_{\rm cl}(t, T) \propto \xi(t, T)^3$, the experimental data can be fitted using, for the correlation length, a power law with a small exponent with a linear T dependence, or activated dynamics, i.e., a logarithm elevated to a power of order 5. Baity-Jesi *et al.* [19] used the same type of analysis as [28] to obtain the cluster size from large-scale simulations of the $J = \pm 1$ EA model. They also express the cluster size in terms of a correlation length elevated to a power.

To conclude, our average cluster size features a slow systematic increase with time that can be fitted by both a logarithm and a power law, in broad agreement with previous findings. The correlation length, for which we do not have direct results, is known to have a qualitatively similar growth. The precise connection between cluster size and correlation length needs, we believe, further numerical verification.

IV. SUMMARY AND CONCLUSIONS

Spin-glass phenomenology is experimentally well described [2,3], while much theoretical understanding relies on partly competing approaches, conceptually rooted in equilibrium statistical mechanics. The ambition of record dynamics (RD) is to offer a simple and general coarse-graining method to analyze the dynamics of a class of metastable systems, to which spin glasses belong.

In this work, log-time homogeneity and the ensuing RD predictions for the decay of the excess energy and the TRM are verified in a spin-glass thermoremanent magnetization numerical simulation.

In thermal equilibrium, spontaneous fluctuations and linear response convey the same dynamical information, since the initial state of a linear response experiment could also have arisen from a spontaneous fluctuation. The situation is more complicated in a TRM setting, because the barrier structure controlling the dynamics depends on the external magnetic field [28,37]. Barrier climbing has a temperature dependence described by a temperature scaling exponent. The latter is $\alpha = 1$ for the TRM data, as expected from quasiequilibrium

fluctuations, but $\alpha = 1.75$ for spontaneous fluctuation, a value explained in [20] in terms of the density of states near local energy minima. Apart from this difference, the present results concur with Ref. [20]. This, combined with the agreement with both experimental and other numerical results, confirms the validity of the WTM as a simulational tool.

Finally, we show that the size of spin clusters overturned by quakes grows logarithmically in time, in agreement with [20]. Wood [36] collects correlation length data of different origins, and shows that they all can be fitted by a power law with a small exponent, linearly dependent on the temperature. We doubt that the correlation length and the cluster size have a simple geometric relation. Furthermore, considering that the correlation length typically only varies over less than a decade, the difference between a power law and a logarithm is moot, and the correlation length could well grow logarithmically in time.

To conclude, together with Ref. [20] this work buttresses a RD description of complex dynamics, and it confirms that the WTM algorithm, upon which our data analysis relies, generates a Markov chain in configuration space that closely mimics the dynamics of experimental systems.

ACKNOWLEDGMENT

P.S. thanks Stefan Boettcher for interesting conversations on record dynamics and for his comments on this work.

[1] E. Vincent, J. Hammann, M. Ocio, J.-P. Bouchaud, and L. F. Cugliandolo, Slow dynamics and aging in spin-glasses, in *Complex Behaviour of Glassy Systems*, edited by M. Rubí and C. Pérez-Vicente, Lecture Notes in Physics Vol. 492 (Springer, Berlin, Heidelberg, 1997), pp. 184–219.

[2] P. Nordblad and P. Svedlindh, Experiments on spin glasses, in *Spin Glasses and Random Fields*, edited by A. P. Young (World Scientific, Singapore, 1997), p. 1.

[3] E. Vincent, Ageing, rejuvenation and memory: The example of spin glasses, Lect. Notes Phys. **716**, 7 (2007).

[4] G. L. Hunter and E. R. Weeks, The physics of the colloidal glass transition, Rep. Prog. Phys. **75**, 066501 (2012).

[5] P. Sibani and C. Svaneborg, Dynamics of dense hard sphere colloidal systems: A numerical analysis, Phys. Rev. E **99**, 042607 (2019).

[6] M. Nicodemi and H. J. Jensen, Aging and memory phenomena in magnetic and transport properties of vortex matter: A brief review, J. Phys. A **34**, 8425 (2001).

[7] N. Becker, P. Sibani, S. Boettcher, and S. Vivek, Temporal and spatial heterogeneity in aging colloids: A mesoscopic model, J. Phys.: Condens. Matter **26**, 505102 (2014).

[8] A. E. Nicholson and P. Sibani, Cultural evolution as a non-stationary stochastic process, Complexity **21**, 214 (2016).

[9] R. Arthur, A. Nicholson, P. Sibani, and M. Christensen, The tangled nature model for organizational ecology, Comput. Math. Organ Theor. **23**, 1 (2016).

[10] M. Alba, M. Ocio, and J. Hammann, Ageing process and response function in spin glasses: An analysis of the thermoremanent magnetization decay in Ag:Mn(2.6%), Europhys. Lett. **2**, 45 (1986).

[11] V. S. Zotev, G. F. Rodriguez, G. G. Kenning, R. Orbach, E. Vincent, and J. Hammann, Role of initial conditions in spin-glass aging experiments, Phys. Rev. B **67**, 184422 (2003).

[12] E. Vincent, Slow dynamics in spin glasses and other complex systems, in *Recent Progress in Random Magnets*, edited by D. H. Ryan (McGill University Press, Montreal, Canada, 1992), pp. 209–246.

[13] G. F. Rodriguez, G. G. Kenning, and R. Orbach, Full Aging in Spin Glasses, Phys. Rev. Lett. **91**, 037203 (2003).

[14] G. G. Kenning, G. F. Rodriguez, and R. Orbach, End of Aging in a Complex System, Phys. Rev. Lett. **97**, 057201 (2006).

[15] H. Rieger, Non-equilibrium dynamics and aging in the three dimensional Ising spin-glass model, J. Phys. A **26**, L615 (1993).

[16] J. Kisker, L. Santen, M. Schreckenberg, and H. Rieger, Off-equilibrium dynamics in finite-dimensional spin-glass model, Phys. Rev. B **53**, 6418 (1996).

[17] P. Sibani, Linear response in aging glassy systems, intermittency and the Poisson statistics of record fluctuations, Eur. Phys. J. B **58**, 483 (2007).

[18] F. Belletti, A. Cruz, L. A. Fernandez, A. Gordillo-Guerrero, M. Guidetti, A. Maiorano, F. Mantovani, E. Marinari, V. Martin-Mayor, J. Monforte, A. Muñoz Sudupe, D. Navarro, G. Parisi, S. Perez-Gaviro, J. J. Ruiz-Lorenzo, S. F. Schifano, D. Sciretti, A. Tarancon, R. Tripiccione, and D. Yllanes (Janus Collaboration), An in-depth view of the microscopic dynamics of Ising spin glasses at fixed temperature, J. Stat. Phys. **135**, 1121 (2009).

[19] M. Baity-Jesi, E. Calore, A. Cruz, L. A. Fernandez, J. M. Gil-Narvion, A. Gordillo-Guerrero, D. Iñiguez, A. Maiorano, E. Marinari, V. Martin-Mayor, J. Monforte-Garcia, A. Muñoz-Sudupe, D. Navarro, G. Parisi, S. Perez-Gaviro, F. Ricci-Tersenghi, J. J. Ruiz-Lorenzo, S. F. Schifano, B. Seoane, A. Tarancon, R. Tripiccione, and D. Yllanes (Janus Collaboration), Matching Microscopic and Macroscopic Responses in Glasses, Phys. Rev. Lett. **118**, 157202 (2017).

[20] P. Sibani and S. Boettcher, Mesoscopic real-space structures in spin-glass aging: The Edwards-Anderson model, Phys. Rev. B **98**, 054202 (2018).

[21] S. F. Edwards and P. W. Anderson, Theory of spin glasses, J. Phys. F **5**, 965 (1975).

[22] P. Anderson, H. J. Jensen, L. P. Oliveira, and P. Sibani, Evolution in complex systems, Complexity **10**, 49 (2004).

[23] P. Sibani, Mesoscopic fluctuations and intermittency in aging dynamics, Europhys. Lett. **73**, 69 (2006).

[24] P. Sibani, Coarse-graining complex dynamics: Continuous time random walks vs. record dynamics, Europhys. Lett. **101**, 30004 (2013).

[25] R. G. Palmer, Broken ergodicity, Adv. Phys. **31**, 669 (1982).

[26] P. Sibani, G. F. Rodriguez, and G. G. Kenning, Intermittent quakes and record dynamics in the thermoremanent magnetization of a spin-glass, Phys. Rev. B **74**, 224407 (2006).

[27] J. Dall and P. Sibani, Faster Monte Carlo simulations at low temperatures. The waiting time method, Comput. Phys. Commun. **141**, 260 (2001).

[28] Y. G. Joh, R. Orbach, G. G. Wood, J. Hammann, and E. Vincent, Extraction of the Spin Glass Correlation Length, Phys. Rev. Lett. **82**, 438 (1999).

[29] H. G. Katzgraber, M. Körner, and A. P. Young, Universality in three-dimensional Ising spin glasses: A Monte Carlo study, Phys. Rev. B **73**, 224432 (2006).

[30] H. G. Katzgraber and A. P. Young, Monte Carlo studies of the one-dimensional Ising spin glass with power-law interactions, Phys. Rev. B **67**, 134410 (2003).

[31] S. Boettcher, D. M. Robe, and P. Sibani, Aging is a log-Poisson process, not a renewal process, Phys. Rev. E **98**, 020602(R) (2018).

[32] P. Sibani, J. M. Pedersen, K. H. Hoffmann, and P. Salamon, Monte Carlo dynamics of optimization problems, a scaling description, Phys. Rev. A **42**, 7080 (1990).

[33] C. Uhlig, K. H. Hoffmann, and P. Sibani, Relaxation in self similar hierarchies, Z. Phys. B **96**, 409 (1995).

[34] P. Sibani and J.-O. Andersson, Excitation morphology in short range Ising spin glasses, Physica A **206**, 1 (1994).

[35] J.-O. Andersson and P. Sibani, Domain growth and thermal relaxation in spin glasses, Physica A **229**, 259 (1996).

[36] G. G. Wood, The spin glass correlation length and the crossover from three to two dimensions, J. Magn. Magn. Mater. **322**, 1775 (2010).

[37] S. Guchhait and R. L. Orbach, Magnetic Field Dependence of Spin Glass Free Energy Barriers, Phys. Rev. Lett. **118**, 157203 (2017).